Available online at www.sciencedirect.com
SCIENCE DIRECT
Fluid Phase Equilibria 242 (2006) 169–175
FLUID PHASE EQUILIBRIA
www.elsevier.com/locate/fluid

Vapor–liquid equilibria for the ternary system of carbon dioxide + ethanol + ethyl acetate at elevated pressures

Chen-Hsi Cheng, Yan-Ping Chen *

Department of Chemical Engineering, National Taiwan University, Taipei, Taiwan, ROC

Received 8 September 2005; received in revised form 18 January 2006; accepted 25 January 2006

Abstract

Vapor–liquid equilibrium (VLE) data for the ternary system of carbon dioxide, ethanol and ethyl acetate were measured in this study at 303.2, 308.2, and 313.2 K, and at pressures from 4 to 7 MPa. A static type phase equilibrium apparatus with visual sapphire windows was used in the experimental measurements. New VLE data for CO_2 in the mixed solvent were presented. These ternary VLE data at elevated pressures were also correlated using either the modified Soave–Redlich–Kwong or Peng–Robinson equation of state, with either the van der Waals one-fluid or Huron–Vidal mixing model. Satisfactory correlation results are reported with temperature-independent binary parameters. It is observed that at 313.2 K and 7 MPa, ethanol can be separated from ethyl acetate into the vapor phase at all concentrations in the presence of high pressure CO_2.

Keywords: Experimental data; VLE; Ternary system

1. Introduction

Supercritical carbon dioxide is widely used in extraction, reaction and separation to minimize the amount of traditionally required organic solvents. For example, supercritical CO_2 was used for the enzymatic reaction and, at the same time, in the product recovery by extraction [1]. Phase equilibrium data are thus important for the fluid mixtures involving supercritical CO_2. In recent literature, the esterification of acetic acid with ethanol to form ethyl acetate was investigated using supercritical CO_2 [2,3]. Table 1 lists the data sources for vapor–liquid equilibrium (VLE) of ternary systems involving high pressure CO_2, alcohol and ester compounds. It is indicated [4,5] that ternary VLE data for such systems are still inadequate, more experimental data are required for engineering applications. We have measured the VLE data for CO_2 and esters using either the semi-flow or static apparatus [6,7] at pressures up to 13 MPa. We extend our previous work to ternary systems of CO_2 with ethanol and ethyl acetate in this study. Using supercritical CO_2, the esterification of acetic acid with ethanol can be a green process with less amount of acid catalyst [3]. VLE data for the binary, ternary and four-component mixtures in this reaction process are useful for the chemical process design and separation of products due to the supercritical extraction effect. It is also shown in Table 1 that the ternary VLE data for supercritical CO_2 with ethanol and ethyl acetate are not yet available in literature. We intend to measure these VLE data and investigate the appropriate conditions that the esterification reaction products can be separated due to the supercritical extraction effect without the formation of the azeotropic compound. The experimental measurements of this study were carried out at temperatures of 303.2, 308.2, and 313.2 K, with the pressures range from 4 to 7 MPa. The measured data were also correlated using the equation of state (EOS) method. The modified Soave–Redlich–Kwong EOS [8] and the widely used Peng–Robinson EOS [9] were employed in the correlation. The van der Waals one-fluid (VDW1) mixing model and the Huron–Vidal mixing model [10] were applied in the correlation. The optimally fitted binary interaction parameters are presented and the accuracies of correlated results from these models are compared.

2. Experimental

2.1. Chemicals

High pressure liquefied carbon dioxide with purity more than 99.9 mass% was available from San-Fu Chemical Co. (Taiwan).

* Corresponding author. Fax: +886 2 2362 3040.
E-mail address: ypchen@ntu.edu.tw (Y.-P. Chen).

0378-3812/$ – see front matter © 2006 Elsevier B.V. All rights reserved.
doi:10.1016/j.fluid.2006.01.017

Table 1
List of the VLE data for CO_2 (1) + X (2) + Y (3) ternary systems in recent literature

X	Y	P (MPa)	T (K)	Reference
Ethanol	Methanol	2.0–8.0	313.2	[11]
Ethanol	*p*-Cresol	10.0–30.0	373.2	[24]
Ethanol	*o*-Cresol	10.0–20.0	373.2	[24]
1-Dodecanol	1-Hexadecanol	25.0–30.0	393.2	[25]
Ethanol	α-Tocochromanol	17.0	343.2	[26]
m-Cresol	Phenol	8.0–40.0	308.2	[27]
o-Cresol	*p*-Cresol	15.0–31.0	323.2–373.2	[24]
Methanol	2-Methyl-2-butanol	2.0–8.2	313.2	[28]
2-Butanol	Vinyl acetate	0.9–14.0	278.2–510.2	[5]
α-Cyano-*m*-phenoxybenzyl alcohol	α-Cyano-*m*-phenoxybenzyl acetate	20.0	313.2	[1]
1-Octanol	α-Cyano-*m*-phenoxybenzyl acetate	9.4–16.2	313.2	[1]
Methyl oleate	Methyl linoleate	4.7–21.0	313.2–333.2	[29]
Ethyl acetate	Isoamyl acetate	6.0	333.2	[18]
Acetic acid	Ethanol	7.4–17.4	304.5–547.7	[4]
Acetic acid	Water	7.0–17.0	313.0–433.0	[30,31]
Ethanol	Water	8.1–18.5	313.2–343.2	[14,21]
Ethyl acetate	Water	7.1–14.9	304.5–546.2	[4]

Absolute GR grade ethanol was purchased from Fisher Scientific Co. and its purity was better than 99.99 mass% from the gas chromatograph (GC) test. Ethyl acetate was purchased from Merck Co. and its purity was better than 99.8 mass% from the GC test. No water content was detected from the GC analyses. These chemicals were used without further purification. The properties of pure ethanol and ethyl acetate were measured in this study and the results are shown in Table 2. The refractive indices were measured at 293.2 ± 0.1 K using an Abbe refractometer, Atago 3T, with an accuracy of ±0.0001. The densities of pure compounds were measured at 293.2 ± 0.1 K using the Anton Paar DMA 58 density meter with an accuracy of ±0.1 kg/m^3. From the comparison with literature values shown in Table 2, the purities of pure chemicals are acceptable for VLE measurements.

2.2. Apparatus

The phase equilibrium apparatus has been described in our previous work [7]. It was a static-type apparatus in which the coexisting phases were recirculated, sampled, and analyzed. The apparatus mainly consists of three sections for the input of samples, the high pressure equilibrium cell, and the analyses of the compositions in the equilibrium phases. The equilibrium cell has an internal volume of 320 mL, with three pairs of visual sapphire windows (Sitec, Switzerland) for visual observation of the phase behavior. The pressure in the equilibrium cell was measured by a Druck gauge (PDCR-4031, up to 700 bar) with a digital indicator (DPI-281). The temperature of the equilibrium cell was measured by a K-type thermocouple with the resolution of 0.01 K. The accuracies for the temperature and pressure measurements in our experimental ranges are ±0.1 K and ±0.01 MPa, respectively. The liquid phase in the cell was recirculated using a magnetic pump (Micropump, series 180-HP) to reach phase equilibrium. The vapor sampling valve (Valco, 6UW) and the liquid sampling valve (Rheodyne, 7010) were used in this study. The GC (Shimadzu, 14B) column was packed with Porapak P. It was equipped with a thermal conductivity detector (TCD) for on-line analyses. Helium was used as the carrier gas with a flow rate of 45 mL/min. The temperatures for the TCD and the GC column were kept at 483.2 and 413.2 K, respectively. The equilibrium cell and sampling valves were all immersed in a water bath where the temperature was controlled at the desired value ±0.1 K. Heating tapes were used in the sampling line to avoid any condensation.

2.3. Calibration procedures

The volumes of the sampling loops were calibrated in this study using distilled water controlled at 298.2 K by following the similar procedures shown in literature [11,12]. The volumes were determined as 21.83 and 4.52 μL for the vapor and liquid sampling loops, respectively.

The calibration of GC was made by plotting the peak areas against the number of moles of the pure gas or liquid sample, as shown in previous literature [13,14]. For the liquid samples, a digital balance (Mettler Toledo AX105, with accuracy of 2 ± 10^{-5} g) was used to evaluate the weight and number of moles. The GC peak areas for ethanol and ethyl acetate were

Table 2
Comparison of the measured refractive indices and densities for pure compounds with literature data

Compound	n^D (T = 293.2 K)		ρ (kg m^{-3}, T = 293.2 K)		GC purity (mass%)
	Experimental	Literature	Experimental	Literature	
Ethanol	1.3600	1.3594 [32]	789.5	789.4 [33]	>99.99
Ethyl acetate	1.3702	1.3704 [32]	900.6	900.6 [32]	>99.80

plotted against their number of moles, and the third order polynomial curves were found satisfactory for the calibration of these pure liquid samples. Calibrations for the gas samples were performed when carbon dioxide was pressurized to a desired value at a given temperature. With the gas sampling valves connected to GC, the peak areas were obtained at various T and P conditions. The molar volumes for carbon dioxide at various T and P were obtained using the data base of NIST [15]. The third order polynomial curves were again found satisfactory at various isotherms for gas phase calibrations.

2.4. Experimental procedures

The experimental apparatus was firstly evacuated using a vacuum pump. The liquid mixture of ethanol and ethyl acetate at a specific composition (ethanol mole fractions of 0.7143, 0.6667, 0.6, 0.5 and 0.2857) was degassed for 20 min before charging into the equilibrium cell that was immersed in a water bath. Carbon dioxide was then fed into the system through a high pressure pump until the system reached a desired pressure. The liquid phase mixture was recirculated using a magnetic pump at a flow rate of 320 mL/min in order to enhance rapid phase equilibrium. At all experimental conditions, the equilibrium vapor and liquid phases were visually observed through the windows of the cell after 0.5 h of recirculation. The system was then settled for 3.5 h to reach the final equilibrium state. The final pressure was then recorded and the equilibrium compositions of the two phases were analyzed using GC. The equilibrium compositions were the averaged values of at least five repeated measurements. The sampling loops were then evacuated to remove any residual. The reproducibility for the measured vapor and liquid mole fractions were estimated to be ±0.0001 and ±0.0002, respectively.

2.5. VLE calculation models

The experimentally measured VLE data were further correlated using the equation of state (EOS) models. The equal fugacity criterion was employed where the fugacity for each component in the equilibrium phases was calculated using the cubic type EOS. It has been presented by Chrisochoou et al. [1] that the modified Soave–Redlich–Kwong (MSRK) EOS [8] can satisfactorily correlate the ternary and multicomponent VLE data for systems of the transesterification process involving supercritical CO_2 using only the binary interaction parameters determined from binary VLE data. It is intended to justify their conclusion for the ternary VLE data measured in this study. Besides the MSRK EOS, the widely used Peng–Robinson (PR) EOS [9] was also employed in correlating our experimental results. The MSRK EOS has the following form:

$$P = \frac{RT}{v-b} - \frac{a}{v(v+b)} \tag{1}$$

$$a = 0.42748\frac{R^2 {T_c}^2}{P_c}\alpha(T) \tag{2}$$

$$b = 0.08664\frac{RT_c}{P_c} \tag{3}$$

Table 3
Pure component properties used in this study

Component	T_c [34] (K)	P_c [34] (bar)	ω [34]	m [18]	n [18]
Carbon dioxide	304.19	73.82	0.228	0.6605	0.2054
Ethanol	516.25	63.84	0.637	1.1639	0.3923
Ethyl acetate	523.20	38.30	0.361	0.7460	0.3189

$$\alpha(T) = 1 + (1 - T_r)\left(\frac{m+n}{T_r}\right) \tag{4}$$

where the parameters m and n are available for many pure fluids [8]. The PR EOS has the following form:

$$p = \frac{RT}{v-b} - \frac{a}{v(v+b)+b(v-b)} \tag{5}$$

$$a = 0.45724\frac{R^2 {T_c}^2}{P_c}\alpha(T) \tag{6}$$

$$b = 0.07780\frac{RT_c}{P_c} \tag{7}$$

$$\alpha(T) = \left[1 + (0.37464 + 1.54226\omega - 0.26992\omega^2)\left(1 - \sqrt{\frac{T}{T_c}}\right)\right]^2 \tag{8}$$

The EOS parameters were determined from the constants of pure fluids that are listed in Table 3. For mixture calculations, the following mixing models were employed. For the van der Waals one-fluid (VDW1) mixing model, the EOS parameters were determined by:

$$a_m = \sum\sum x_i x_j (a_i a_j)^{0.5}(1 - k_{ij}) \tag{9}$$

$$b_m = \sum x_i b_i \tag{10}$$

where k_{ij} is the binary interaction parameter and was determined by regressing the experimental VLE data. Another mixing model presented by Huron and Vidal [10] was also used in this study. In this mixing model, the excess Gibbs energy calculated from an EOS is set equal to that from an activity coefficient model at an infinite pressure limit. Applying the NRTL activity coefficient model [16], the EOS parameters were evaluated by the following equations:

$$a_m = b_m \sum_{i=1}^{n} x_i \times \left[\frac{a_i}{b_i} - \frac{1}{\ln 2}\left(\frac{\sum_{j=1}^{n} x_j C_{ji} b_j \exp(-\alpha_{ji} C_{ji}/(RT))}{\sum_{j=1}^{n} x_j b_j \exp(-\alpha_{ji} C_{ji}/(RT))}\right)\right] \tag{11}$$

$$b_m = \sum_{i=1}^{n} x_i b_i \tag{12}$$

where the non-randomness factor α was taken as 0.3 in our correlation. The binary parameters C_{ij} and C_{ji} in the NRTL model were determined by regressing the experimental VLE data.

Table 4
The correlation results for the VLE data of binary systems using the PR and the MSRK EOS with the VDW1 mixing model

EOS	T (K)	P (MPa)	k_{12}	AADx_1 (%)	AADy_1 (%)	Total points	Reference
CO_2 (1) + ethanol (2)							
PR	304.2–308.2	3.75–7.67	0.084	0.43	0.10	11	[17]
MSRK	304.2–308.2	3.75–7.67	0.080	0.40	0.11	11	[17]
CO_2 (1) + ethyl acetate (2)							
PR	313.2	0.92–7.88	−0.016	0.87	0.15	10	[18]
MSRK	313.2	0.92–7.88	−0.019	0.88	0.17	10	[18]
Ethyl acetate (1) + ethanol (2)							
PR	313.2–333.2	0.02–0.64	0.021	0.02	5.43	37	[19]
MSRK	313.2–333.2	0.02–0.64	0.024	0.02	5.55	37	[19]

AAD$x_1 = (100/N)\sum|(x_1^{cal} - x_1^{exp})/x_1^{exp}|$; AAD$y_1 = (100/N)\sum|(y_1^{cal} - y_1^{exp})/y_1^{exp}|$, where N is the number of data points.

We have correlated the VLE data shown in literature [17–19] for three binary systems of CO_2 + ethanol, CO_2 + ethyl acetate and ethyl acetate + ethanol. The optimally fitted temperature-independent binary interaction parameters in either the VDW1 or Huron–Vidal mixing model were evaluated through flash calculation by minimizing the following objective function:

$$\text{obj} = \sum_{i=1}^{n}[|(y_i^{cal} - y_i^{exp})| + |(x_i^{cal} - x_i^{exp})|] \quad (13)$$

The correlation results are shown in Tables 4 and 5 for the VDW1 or Huron–Vidal mixing model, respectively. Generally, both the MSRK and PR EOS yield the comparable accuracy in correlating the binary VLE data. The Huron–Vidal mixing model with the NRTL activity coefficient model has two adjustable parameters, and presents relatively superior results to those from the simple VDW1 mixing model with only a single parameter. These optimally fitted binary interaction parameters were directly applied in predicting the ternary VLE results and comparing with the experimental measured data.

3. Results and discussion

The measured VLE data in this study for the ternary system CO_2 (1) + ethanol (2) + ethyl acetate (3) at 303.2, 308.2, and 313.2 K are presented in Tables 6–8, respectively. Five compositions for ethanol in the feed of ethanol + ethyl acetate were included for each isotherm in the experiments. For each feed composition, VLE data were measured at the given temperature and at four pressures ranging from 4 to 7 MPa. It is observed that the vapor phase is mainly CO_2 with mole fraction >0.99. The mole fractions of ethanol and ethyl acetate in

Table 6
Vapor–liquid equilibrium data for the ternary system of CO_2 (1) + ethanol (2) + ethyl acetate (3) at T = 303.2 K

P (MPa)	x_1	x_2	x_3	y_1	y_2	y_3
4.14	0.3200	0.5100	0.1700	0.9940	0.0050	0.0010
5.02	0.4261	0.4218	0.1521	0.9950	0.0044	0.0006
6.00	0.5374	0.3191	0.1435	0.9955	0.0041	0.0004
6.92	0.7261	0.2124	0.0615	0.9959	0.0039	0.0002
4.12	0.3262	0.4681	0.2057	0.9938	0.0042	0.0020
5.03	0.4431	0.3720	0.1849	0.9941	0.0041	0.0018
6.04	0.5450	0.2765	0.1785	0.9950	0.0034	0.0016
6.92	0.7593	0.1691	0.0716	0.9958	0.0033	0.0009
4.11	0.4190	0.3481	0.2329	0.9934	0.0039	0.0027
5.02	0.4948	0.2952	0.2100	0.9940	0.0035	0.0025
6.04	0.5651	0.2433	0.1916	0.9945	0.0033	0.0022
6.97	0.7840	0.1276	0.0884	0.9951	0.0029	0.0020
4.19	0.4931	0.2750	0.2319	0.9936	0.0027	0.0037
5.03	0.6063	0.2067	0.1870	0.9938	0.0025	0.0037
6.03	0.6240	0.1960	0.1800	0.9943	0.0023	0.0034
7.03	0.8166	0.1040	0.0794	0.9948	0.0018	0.0034
4.16	0.6883	0.1000	0.2117	0.9939	0.0010	0.0051
5.09	0.7264	0.0970	0.1766	0.9942	0.0010	0.0048
6.09	0.8250	0.0800	0.0950	0.9947	0.0008	0.0045
7.03	0.8806	0.0450	0.0744	0.9954	0.0006	0.0040

Table 5
The correlation results for the VLE data of binary systems using the PR and the MSRK EOS with the Huron–Vidal mixing model

EOS	T (K)	P (MPa)	α	C_{12} (J/mol)	C_{21} (J/mol)	AADx_1 (%)	AADy_1 (%)	Total points	Reference
CO_2 (1) + ethanol (2)									
PR	304.2–308.2	3.75–7.67	0.3	4759.95	−495.42	0.36	0.10	11	[17]
MSRK	304.2–308.2	3.75–7.67	0.3	3641.27	−4536.05	0.33	0.11	11	[17]
CO_2 (1) + ethyl acetate (2)									
PR	313.2	0.92–7.88	0.3	−1469.44	1387.55	0.43	0.15	10	[18]
MSRK	313.2	0.92–7.88	0.3	391.98	72.96	0.59	0.17	10	[18]
Ethyl acetate (1) + ethanol (2)									
PR	313.2–333.2	0.02–0.64	0.3	2049.93	4336.29	0.01	2.18	37	[19]
MSRK	313.2–333.2	0.02–0.64	0.3	2053.90	4334.81	0.01	2.17	37	[19]

AAD$x_1 = (100/N)\sum|(x_1^{cal} - x_1^{exp})/x_1^{exp}|$; AAD$y_1 = (100/N)\sum|(y_1^{cal} - y_1^{exp})/y_1^{exp}|$, where N is the number of data points.

Table 7
Vapor–liquid equilibrium data for the ternary system of CO_2 (1) + ethanol (2) + ethyl acetate (3) at $T = 308.2$ K

P (MPa)	x_1	x_2	x_3	y_1	y_2	y_3
4.16	0.2793	0.5726	0.1481	0.9934	0.0055	0.0011
5.02	0.3828	0.4860	0.1312	0.9940	0.0050	0.0010
6.08	0.4815	0.4140	0.1045	0.9949	0.0042	0.0009
6.97	0.6400	0.3000	0.0600	0.9953	0.0039	0.0008
4.15	0.2977	0.5010	0.2013	0.9930	0.0049	0.0021
5.04	0.4204	0.4054	0.1742	0.9938	0.0042	0.0020
6.04	0.5366	0.3004	0.1630	0.9945	0.0039	0.0016
6.96	0.6338	0.2434	0.1228	0.9949	0.0037	0.0014
4.15	0.3110	0.4134	0.2756	0.9927	0.0040	0.0033
5.02	0.4558	0.2953	0.2489	0.9933	0.0036	0.0031
6.09	0.5863	0.2168	0.1969	0.9940	0.0031	0.0029
6.98	0.6876	0.1703	0.1421	0.9945	0.0028	0.0027
4.19	0.5446	0.1706	0.2848	0.9925	0.0030	0.0045
5.09	0.6628	0.1295	0.2077	0.9930	0.0028	0.0042
6.10	0.7948	0.0792	0.1260	0.9936	0.0024	0.0040
6.98	0.8582	0.0532	0.0886	0.9943	0.0019	0.0038
4.16	0.7100	0.0500	0.2400	0.9920	0.0010	0.0070
5.09	0.7900	0.0400	0.1700	0.9930	0.0010	0.0060
6.09	0.8500	0.0400	0.1100	0.9932	0.0009	0.0059
6.99	0.8966	0.0300	0.0734	0.9942	0.0008	0.0050

Table 8
Vapor–liquid equilibrium data for the ternary system of CO_2 (1) + ethanol (2) + ethyl acetate (3) at $T = 313.2$ K

P (MPa)	x_1	x_2	x_3	y_1	y_2	y_3
4.11	0.2230	0.6280	0.1490	0.9890	0.0092	0.0018
5.05	0.3145	0.5450	0.1405	0.9900	0.0088	0.0012
6.07	0.4224	0.4641	0.1135	0.9903	0.0086	0.0011
7.06	0.5396	0.3514	0.1090	0.9904	0.0085	0.0011
4.18	0.2300	0.5590	0.2110	0.9874	0.0089	0.0037
5.08	0.3682	0.4562	0.1756	0.9880	0.0085	0.0035
6.04	0.4634	0.3689	0.1677	0.9890	0.0080	0.0030
7.07	0.5600	0.2902	0.1498	0.9893	0.0079	0.0028
4.16	0.3000	0.4230	0.2770	0.9873	0.0075	0.0052
5.08	0.4000	0.3500	0.2500	0.9874	0.0075	0.0051
6.02	0.5500	0.2500	0.2000	0.9877	0.0075	0.0048
7.07	0.6006	0.2160	0.1834	0.9878	0.0074	0.0048
4.13	0.4718	0.2773	0.2509	0.9876	0.0050	0.0074
5.03	0.5456	0.2428	0.2116	0.9885	0.0050	0.0065
6.04	0.6600	0.1600	0.1800	0.9890	0.0049	0.0061
6.98	0.7400	0.1000	0.1600	0.9895	0.0047	0.0058
4.15	0.5957	0.1619	0.2424	0.9878	0.0037	0.0085
5.09	0.6892	0.1279	0.1829	0.9900	0.0021	0.0079
6.06	0.7915	0.0786	0.1299	0.9905	0.0019	0.0076
6.98	0.8969	0.0212	0.0819	0.9910	0.0019	0.0071

the vapor phase increase with temperature and decrease with pressure.

The optimally fitted binary interaction parameters obtained from correlating the binary mixtures were directly used to predict the VLE results for the ternary system. The calculation results, however, are not satisfactory as shown in Table 9. One possible reason is that the VLE data for the binary mixture of ethyl acetate + ethanol were at a low pressure range. If the binary interaction parameter for ethyl acetate + ethanol was taken as the only adjustable parameter in fitting the ternary VLE data, acceptable results are obtained as shown in Table 9. Table 9 also shows that satisfactory correlation results are presented by fitting the temperature-independent binary interaction parameters directly to the ternary VLE data. It is not always possible to obtain a set of binary interaction parameters that could yield accurate prediction for both binary and multicomponent systems. It is indicated in literature [20] that fitting the EOS to the ternary VLE data gives better correlation.

Graphical presentations of the ternary VLE data are shown in Figs. 1 and 2 at 303.2 K and two isobars of 4 and 7 MPa. Fig. 3 shows the VLE data at 7 MPa but at the other temperature of 313.2 K. These three figures show that the liquid compositions of ethanol and ethyl acetate increase with temperature but decrease with pressure. The solid tie lines represent the calculated results using the PR EOS and the VDW1 mixing model with the binary interaction parameters fitted to the ternary VLE data. Satisfactory agreement between the experimental and correlated results is demonstrated.

To illustrate the effect of separation for ethanol (2) and ethyl acetate (3) in the presence of high pressure CO_2, the separation factors $\alpha_{23} = (y_2/x_2)/(y_3/x_3)$ were examined from all experimental results. As discussed in previous literature [21], component 2 can be separated into the vapor phase with α_{23} greater than unity. In our experimental range, the α_{23} values are greater than unity at 313.2 K and 7 MPa over the entire concentration range. As shown in literature [22], a solvent-free $y^* - x^*$ plot was used to

Table 9
Correlation results for the ternary VLE data of CO_2 (1) + ethanol (2) + ethyl acetate (3)

EOS	Mixing model	Predicted results		Adjustment of BIP for (2) + (3)[a]		Fitting BIP to ternary VLE data[b]	
		AADx_1 (%)	AADy_1 (%)	AADx_1 (%)	AADy_1 (%)	AADx_1 (%)	AADy_1 (%)
PR	VDW1	8.95	0.51	1.60	0.19	1.50	0.19
	Huron–Vidal	6.68	0.21	1.55	0.18	1.47	0.19
MSRK	VDW1	9.09	0.53	1.75	0.20	1.53	0.20
	Huron–Vidal	6.69	0.22	1.65	0.19	1.48	0.18

BIP, binary interaction parameters.
[a] PR EOS: $k_{23} = -0.180$, $C_{23} = 0.584$, $C_{32} = 3.000$; MSRK EOS: $k_{23} = -0.166$, $C_{23} = -0.038$, $C_{32} = 1.374$, C_{ij} [=] kJ/mol.
[b] PR EOS: $k_{12} = 0.096$, $k_{13} = -0.009$, $k_{23} = -0.164$, $C_{12} = 12.761$, $C_{21} = 1.050$, $C_{13} = -0.359$, $C_{31} = 2.356$, $C_{23} = 3.412$, $C_{32} = -0.242$; MSRK EOS: $k_{12} = 0.099$, $k_{13} = -0.007$, $k_{23} = -0.144$, $C_{12} = 5.163$, $C_{21} = -0.625$, $C_{13} = 0.285$, $C_{31} = -0.382$, $C_{23} = 14.687$, $C_{32} = 24.256$.

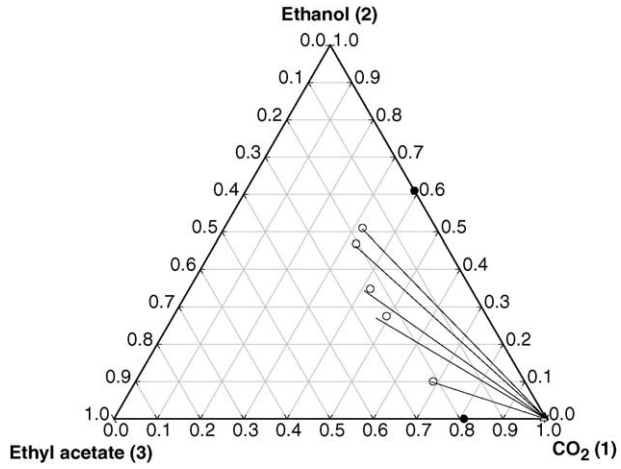

Fig. 1. Vapor–liquid equilibria for carbon dioxide (1) + ethanol (2) + ethyl acetate (3) at $T = 303.2$ K and $P = 4$ MPa (◯, △: mole fractions of the liquid and vapor phases measured in this study; ●: mole fraction of the liquid phase from literature [35,36]).

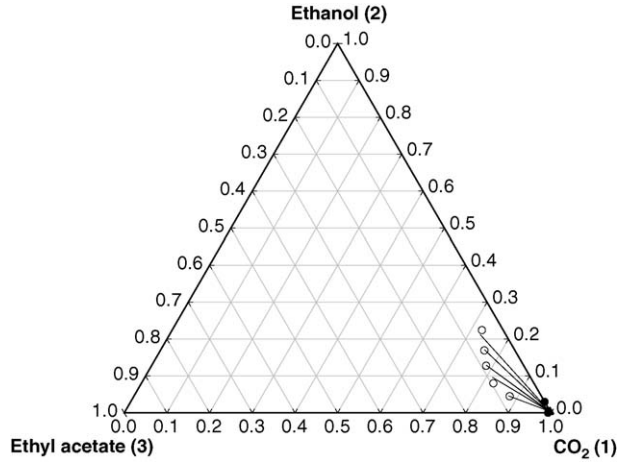

Fig. 2. Vapor–liquid equilibria for carbon dioxide (1) + ethanol (2) + ethyl acetate (3) at $T = 303.2$ K and $P = 7$ MPa (◯, △: mole fractions of the liquid and vapor phases measured in this study; ●: mole fraction of the liquid phase from literature [17,36]).

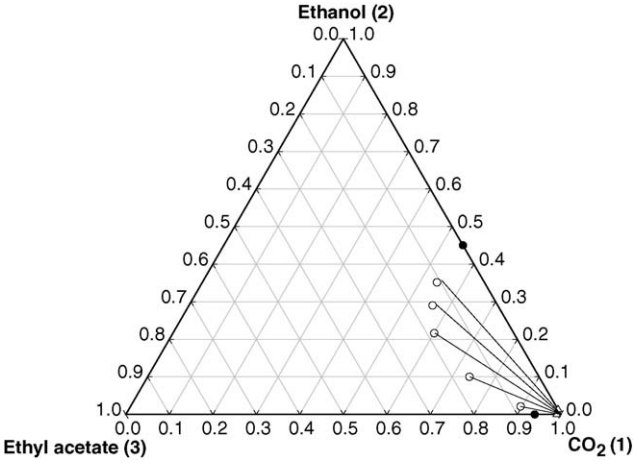

Fig. 3. Vapor–liquid equilibria for carbon dioxide (1) + ethanol (2) + ethyl acetate (3) at $T = 313.2$ K and $P = 7$ MPa (◯, △: mole fractions of the liquid and vapor phases measured in this study; ●: mole fraction of the liquid phase from literature [35,36]).

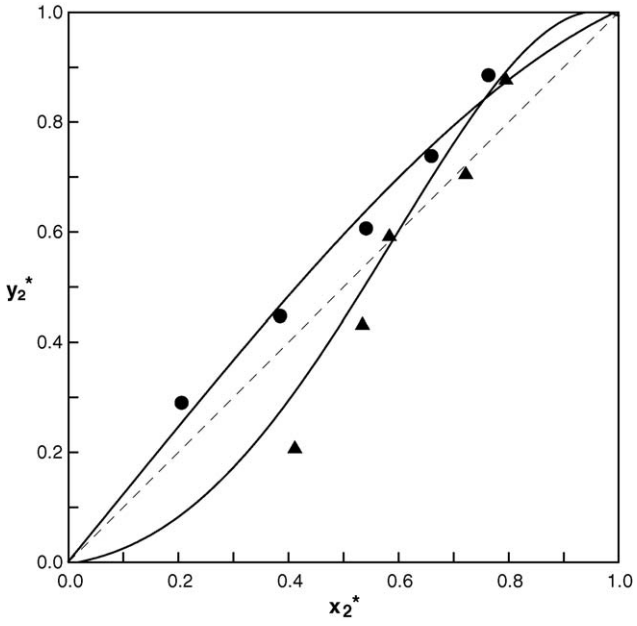

Fig. 4. Plot of the CO_2-free $y_2^* - x_2^*$ curves at 313.2 K for the ternary mixture CO_2 (1) + ethanol (2) + ethyl acetate (3) (experimental data: ▲, $P = 5$ MPa; ●, $P = 7$ MPa; –, calculated results using the PR EOS with the VDW1 mixing model).

illustrate the separation effect. The solvent-free mole fractions are defined as:

$$z_i^* = \frac{n_i}{\sum_{j \neq CO_2} n_j} \tag{14}$$

The plot of the CO_2-free basis ($y_2^* - x_2^*$) curves is shown in Fig. 4 at 313.2 K and at two pressures of 5 and 7 MPa. At atmospheric pressure, the binary mixture of ethanol and ethyl acetate has an azeotrope with ethanol mole fraction of 0.46 [23]. At 313.2 K and 7 MPa, the relative volatility of ethanol to ethyl acetate is greater than unity in the entire composition range and no azeotrope is found. No such separation effect is observed at all concentration range for other temperatures and pressures investigated in this study.

4. Conclusions

Experimental VLE data for the ternary system of carbon dioxide with ethanol and ethyl acetate are reported at 303.2, 308.2, and 313.2 K and pressures from 4 to 7 MPa. The modified Soave–Redlich–Kwong or Peng–Robinson EOS with either the van der Waals one-fluid or Huron–Vidal mixing model were used to correlate the ternary experimental VLE data. With the temperature-independent binary parameters fitted to the ternary VLE data, satisfactory correlation results are obtained for both EOS and mixing models. The experimental data are analyzed on the CO_2-free basis. It is shown that at 313.2 K and 7 MPa, ethanol can be separated from ethyl acetate at all concentrations in the presence of high pressure CO_2.

List of symbols

a, b	parameters in the equation of state
C	binary interaction parameter in the NRTL model
f	fugacity
k	binary interaction parameters in the mixing model
n	number of mole
P	pressure
R	gas constant
T	temperature
x	mole fraction in the liquid phase
y	mole fraction in the vapor phase

Greek letter

α	non-randomness factor in the NRTL model

Subscripts

c	critical properties
i, j	component i or j
m	mixture
r	reduced properties
1, 2	component 1 or 2

Superscripts

cal	calculated value
exp	experimental data
*	CO_2-free basis

Acknowledgement

The authors are grateful to the National Science Council, ROC for supporting this research.

References

[1] A.A. Chrisochoou, K. Schaber, K. Stephen, J. Chem. Eng. Data 42 (1997) 558–561.
[2] L.A. Blanchard, J.F. Brennecke, Green Chem. 3 (2001) 17–19.
[3] Z. Hou, B. Han, X. Zhang, H. Zhang, Z. Liu, J. Phys. Chem. B 105 (2001) 4510–4513.
[4] T. Hu, Z. Qin, G. Wang, X. Hou, J. Wang, J. Chem. Eng. Data 49 (2004) 1809–1814.
[5] R.M.M. Stevens, A. Bakx, P.R.H. van der Neut, T.W. de Loos, J. de Swaan Arons, J. Chem. Eng. Data 42 (1997) 1280–1284.
[6] W.H. Hwu, C.H. Cheng, M. Tang, Y.P. Chen, Fluid Phase Equilib. 215 (2004) 237–244.
[7] C.H. Cheng, Y.P. Chen, Fluid Phase Equilib. 234 (2005) 77–83.
[8] J.A. Sandarusi, A.J. Kidnay, V.F. Yesavage, Ind. Eng. Chem. Process Des. Dev. 25 (1986) 957–963.
[9] D.Y. Peng, D.B. Robinson, Ind. Eng. Chem. Fundam. 15 (1976) 59–64.
[10] M.J. Huron, J. Vidal, Fluid Phase Equilib. 3 (1979) 255–271.
[11] J.H. Yoon, H.S. Lee, H. Lee, J. Chem. Eng. Data 38 (1993) 53–55.
[12] T. Laursen, P. Rasmussen, S.I. Andersen, J. Chem. Eng. Data 47 (2002) 198–202.
[13] K. Suzuki, H. Sue, M. Itou, R.L. Smith, H. Inomata, K. Arai, S. Saito, J. Chem. Eng. Data 35 (1990) 63–66.
[14] J.H. Yoon, H. Lee, B.H. Chung, Fluid Phase Equilib. 102 (1994) 287–292.
[15] http://webbook.nist.gov/chemistry.
[16] H. Renon, J.M. Prausnitz, AIChE J. 14 (1968) 135–144.
[17] S. Takishima, K. Saiki, K. Arai, S. Saito, J. Chem. Eng. Jpn. 19 (1986) 48–56.
[18] A. Chrisochoou, K. Schaber, U. Bolz, Fluid Phase Equilib. 108 (1995) 1–14.
[19] P.S. Murti, M. Van Winkle, Chem. Eng. Data Ser. 3 (1958) 72–81.
[20] R. Ruivo, A. Paiva, P. Simoes, J. Supercrit. Fluids 29 (2004) 77–85.
[21] J.S. Lim, Y.Y. Lee, H.S. Chun, J. Supercrit. Fluids 7 (1994) 219–230.
[22] P. Traub, K. Stephan, Chem. Eng. Sci. 45 (1990) 751–758.
[23] M. Kato, H. Konishi, M. Hirata, J. Chem. Eng. Data 15 (1970) 435–439.
[24] O. Pfohl, A. Pagel, Fluid Phase Equilib. 157 (1999) 53–79.
[25] I.F. Holscher, M. Spee, G.M. Schneider, Fluid Phase Equilib. 49 (1989) 103–113.
[26] A. Birtigh, J. Stoldt, G. Brunner, J. Supercrit. Fluids 8 (1995) 162–166.
[27] G. Di Giacomo, S. Brandani, V. Brandani, G. Del Re, Fluid Phase Equilib. 95 (1994) 313–327.
[28] H.S. Lee, S.Y. Mun, H. Lee, Fluid Phase Equilib. 167 (2000) 131–144.
[29] M. Zou, Z.R. Yu, S.S.H. Rizvi, J.A. Zollweg, J. Supercrit. Fluids 3 (1990) 85–90.
[30] K.M. Dooley, A.W. Cain, F.C. Knopf, J. Supercrit. Fluids 11 (1997) 81–89.
[31] B. Rumpf, J. Xia, G. Maurer, Ind. Eng. Chem. Res. 37 (1998) 2012–2019.
[32] T.E. Daubert, R.P. Danner, Physical and Thermodynamic Properties of Pure Chemicals: Data Compilation, Hemisphere, New York, 1989.
[33] D.R. Lide, H.P.R. Frederikse, CRC Handbook of Chemistry and Physics, 80th ed., CRC Press Inc., Boca Raton, FL, 1999.
[34] B.E. Poling, J.M. Prausnitz, J.P. O'Connell, The Properties of Gas and Liquids, 5th ed., McGraw Hill Inc., New York, 2001.
[35] C.J. Chang, K.L. Chiu, C.Y. Day, J. Supercrit. Fluids 12 (1998) 223–237.
[36] Z. Wanger, J. Pavlicek, Fluid Phase Equilib. 97 (1994) 119–126.